Applied Surface Science 579 (2022) 152144

Contents lists available at ScienceDirect

Applied Surface Science

journal homepage: www.elsevier.com/locate/apsusc

Full Length Article

# Synergistic reinforced superhydrophobic paper with green, durability, and antifouling function

Cai Long [a,b,1], Yongquan Qing [a,b,*,1], Xiao Long [c], Niu Liu [a,b], Xinyu Xu [a,b], Kai An [a,b], Mengxue Han [a,b], Songhe Li [d], Changsheng Liu [a,b]

[a] School of Materials Science and Engineering, Northeastern University, Shenyang 110819, China
[b] Key Laboratory for Anisotropy and Texture of Materials, Ministry of Education, Northeastern University, Shenyang 110819, China
[c] Bohai University, Jinzhou 121013, China
[d] Shenyang Pharmaceutical University, Shenyang 110016, China

ARTICLE INFO

*Keywords:*
Superhydrophobic paper
Green
Durability
Antifouling function

ABSTRACT

Among the various paper-based technologies that exist today, superhydrophobic paper has attracted considerable attention owing to its incredible repellency and antifouling behavior against both water and oil based liquids. However, its practical applications are limited due to its poor durability and the use of fluorochemicals during the preparation process, which are harmful to both humans and environment. Herein, we developed a synergistic reinforced superhydrophobic paper (SRSP) using green-based waxes as an adhesive for grafting hydrophobic nanoparticles, thereby reducing safety and environmental concerns as well as improving durability. The resulting paper exhibits strong durability to sandpaper abrasion, finger-wipe, knife-scratch, tape-peeling, bending, folding, and sustained exposure to corrosion media. Additionally, not only does the SRSP surface directly prevented adhesion of water-based contaminants (e.g., muddy water, coca cola, or milk), but also indirectly repelled solid contaminants (e.g., hydrophilic or hydrophobic particles) upon washing with water, thereby demonstrating highly efficient antifouling ability. Intriguingly, the silicone oil-infused SRSP surface could easily repelled low-surface-energy droplets such as hot water, oil, or fouled oil. It is envisioned that the SRSP developed in this study can find potential applications in microfluidics, recyclable packaging materials, paper-based flexible electronics, and new sophisticated membrane-type materials.

## 1. Introduction

Paper is one of the most important inventions from ancient China, and it is an essential material utilized in diverse fields due to its low cost and scalability, and plays a crucial role in daily-life [1–3]. It is well known that paper is a nonwoven mat composed primarily of cellulose, which is the most abundant natural polymer on earth and is biodegradable, nontoxic, and renewable. However, due to the inherent high hydrophilicity of cellulose, commercial paper is easily wetted by liquids and attached onto the surface by fouling during use, which has a negative impact on daily-life, industries, and potential applications [4–7]. According to reports, superhydrophobic papers are characterized by their remarkable repellency and efficient antifouling performance against water- and oil-based liquids [5–11]. Nevertheless, real-world applications of existing superhydrophobic papers are extremely rare due to poor durability towards mechanical abrasion and chemical corrosion in harsh environments. Moreover, the use of toxic fluorochemicals during the preparation process makes them unattractive from an environmental perspective.

Typically, superhydrophobic surfaces with nano and/or micro-scale structures that support trapped air layer are easily damaged by external forces or changes in the environment, such as wiping, abrasion, and exposure to acid or base conditions [6,12–14]. There were basically three different strategies that have been exployed to address the issue of durability. The first method involved chemical bonds formation between coating molecules and cellulose fibers [4,6,7,15,16], the second implemented an inexpensive, scalable, and universal surface sizing technique [7,17,18], and the third enhanced van der Waals forces through the use of low-surface-energy adhesives [19,20]. Despite notable progress, rather less attention has been paid to the development

* Corresponding author.
*E-mail address:* qingyq@mail.neu.edu.cn (Y. Qing).
[1] Cai Long and Yongquan Qing contributed equally to this work, and are equally considered first authors.

https://doi.org/10.1016/j.apsusc.2021.152144
Received 6 October 2021; Received in revised form 14 November 2021; Accepted 3 December 2021
Available online 7 December 2021

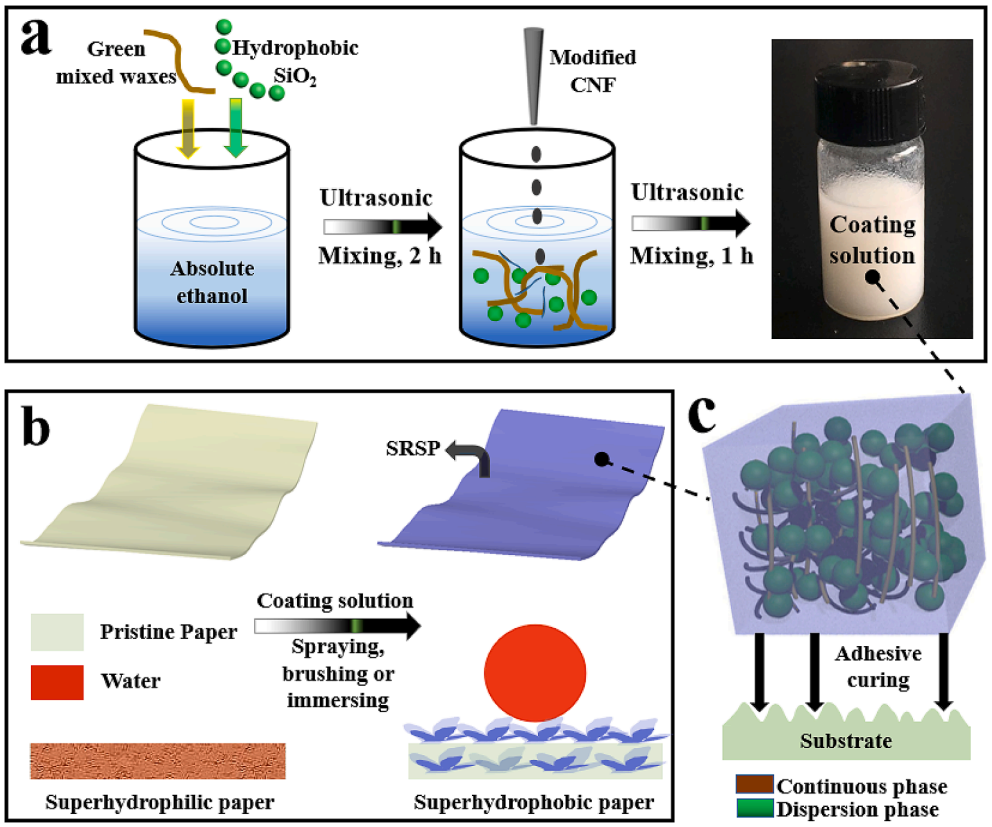


**Fig. 1. Design of SRSP.** (a) Fabrication process schematic illustration of targeted coating solution, and the building block of SRSP. (b) Schematic illustration of the procedure for coating treatment procedure to obtain the SRSP. (c) Illustration of the superhydrophobic composite coating layer (consisting of the continuous phase: brown part and dispersion phase: green part) was formed on the surface of the pristine paper-based substrate through synergistic reinforcement of cross-linking reaction.

of green and renewable superhydrophobic paper.

Furthermore, where chemical modification was required, the superhydrophobic papers were fabricated through the introduction of fluorocarbon functional groups which can effectively reduce surface energy [6,21,22]. Unfortunately, fluorocarbon compounds are toxic and detrimental to our health as they enter the food chain and undergo bioaccumulation in wildlife, causing these fluorocarbon paper difficult to be used in the fields of food packaging, commodities, and medicine [5,23–28]. Besides, most waterproof papers are primarily prepared from non-renewable materials, which is not facilitates the sustainable development of functional paper. The public's ever increasing environmental awareness and stricter regulations make the use of fluorine-free raw materials to prepare superhydrophobic paper an attractive alternative [2,5,20,29–31]. Recent studies have shown the potential of using fatty acids (e.g., stearic acid [32], myristic acid [5]), green-based waxes (e. g., bee wax [20,33,34], carnauba wax [18,31,32]), and cross-linked poly (dimethylsiloxane) [7,29,35] as fluorinated compound alternatives. However, these materials are inherently less water resistant than fluorocarbons, and overall less desirable, especially under prolonged use. For instance, the adhesion force between these substances and paper is extremely weak, which promotes easy detachment of the low-surface-energy chemical component or the entire coating from the paper, and is widely recognized as an unresolved problem [5,36]. Accordingly, it tends to be difficult to simultaneously optimize the durability and eco-friendly for such papers.

Waxes are considered to be easily accessible natural products with good hydrophobic and adhesion properties due to a high content in esters of long-chain fatty alcohols and acids, as well as long-chain alkanes [34,37,38]. In this work, we used low-surface-energy green-based waxes mixture adhesives filled with non-toxic hydrophobic $SiO_2$ nanoparticles to formulate synergistic reinforced superhydrophobic paper (SRSP) that was both green and durable. The key advantage of SRSP design strategy was the absence of fluorochemicals in the preparation process, which adheres to the requirements of sustainable development due to green-based materials. In particular, we have successfully integrated green sustainability, durability, and antifouling performances on pristine paper's surface. Such surface is durable and does not exhibit any deterioration of wettability even under severe conditions, and exhibits its excellent direct and indirect antifouling properties. Additionally, we also demonstrated the extent of water resistance and enhanced integrity of SRSP for use in new sophisticated membrane-type materials, paper-based flexible electronics, currency printing, and recyclable packaging materials. The outstanding performance of the waterproof paper and its completely green preparation for scale-up highlights its potential applicability in both microfluidics and medical fields.

## 2. Experimental

### 2.1. Materials

Nano-$SiO_2$ with an average size of 200–300 nm was provided by Shanghai Aladdin-Reagent Co., Ltd. Oleic acid (OA) was purchased from Sigma-Aldrich. Rice bran wax and candelilla wax were supplied by Dongguang Nan beeswax Industry Co., Ltd. γ-Aminopropyltriethoxysilane (KH550) was obtained from Nanjing Daoning Chemical Co., Ltd. Native cellulose nanofiber (CNF) was purchased from BioPlus. Rapeseed oil (commercial), and absolute ethanol were used as received without any further purification.

### 2.2. Preparation of the SRSP

Rice bran wax (1.5 g) and candelilla wax (0.5 g) were dissolved in ethanol solution (200 mL) under magnetic stirring at 85 °C for 2 h to obtain a clear solution. Subsequently, OA (0.35 mL) and $SiO_2$ particles (1 g) were placed in absolute ethanol (9 mL), and mixed well under vigorous magnetic stirring at 45 °C for 1.5 h to form the hydrophobic $SiO_2$ (OA-$SiO_2$) nanoparticles solution.

The as prepared solutions were thoroughly mixed and then

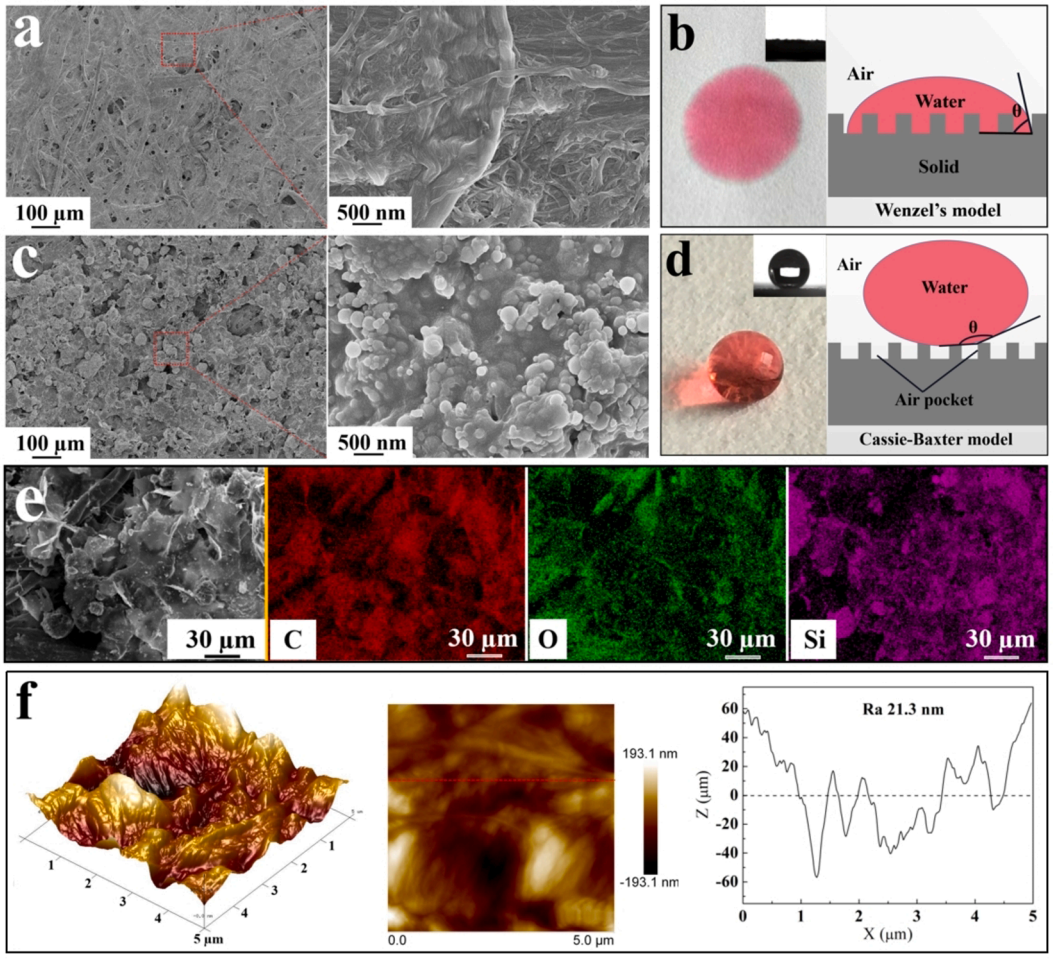


**Fig. 2. Microstructure of the SRSP.** SEM images of (a) the superhydrophilic pristine paper and (c) the SRSP surface at different magnifications. Digital photographs of typical wettability showing water on (b) the superhydrophilic pristine paper and (d) the SRSP surface, and corresponding to the Wenzel and Cassie state (right images), respectively. (e) Elemental mappings of the main elements C, O, and Si of SRSP surface. (f) AFM image of the SRSP surface.

magnetically stirred at 45 °C for 2 h, followed by addition of KH550 modified CNFs (0.4 wt%). Next, this mixture was stirred at 45 °C for 1 h to obtain a uniform milky composite suspension. Finally, the prepared suspension was applied on original paper through spraying, brushing, and immersing, and the resulting samples were left in air for 20 min followed by the oven drying at 75 °C for 2 h to form the SRSP.

Silicone oil was added onto SRSP using a pipette, causing the silicone oil to spread spontaneously, which was locked onto the coating through capillary wicking on the micro/nanostructures, forming a typical slippery liquid-infused SRSP (*SLIPS-SRSP*).

### 2.3. Characterization

The contact angles (CAs) and sliding angles (SAs) of droplets (6–8 μL) were measured using an optical contact angle meter (JCY-2, Fangrui) at room temperature. The surface morphology was characterized using scanning electron microscopy (SEM, Ultra Plus, CarlZeiss AG, Germany), and energy dispersive X-ray spectroscopy (EDS) data were acquired using the same instrument. Surface chemical compositions were characterized using Fourier transform infrared (FTIR) spectroscopy (Vertex70 Bruker, Germany) and X-ray photoelectron spectroscopy (XPS, K-Alpha, United States), respectively. Surface 3D morphology and roughness were investigated using an atomic force microscope (AFM, Multimode Nanoscope IIIa, USA).

## 3. Results and discussion

### 3.1. Strategy for achieving SRSP

We designed the SRSP based on a the multi-alkylation treatment and the synergistic reinforcement as follows. First, the hydrophilic $SiO_2$ as the inorganic phase was dehydrated and alkylated to obtain OA-$SiO_2$, providing hydrophobic source and texture control (Fig. S1a). Second, heavy crosslinking was incorporated, which was essential to liquid repellency, where insufficient crosslinking density tended promote inferior liquid repellency and surface reconstruction [39]. Thus, to provide adequate crosslinking sites and to enhance liquid repellency, the green and renewable rice bran/candelilla mixed waxes (other food grade edible waxes can also be considered in future research) were selected as binders owing to their strong adhesion properties and the presence of abundant low-surface-energy alkyl groups [37]. Next, the waxes were added to ethanol solution and dispersed using ultrasonic cell breakage to form a heavy crosslinking sol (Fig. 1a). Third, the native hydrophilic CNFs were chemically alkylated with KH550 to enhance the hydrophobicity and mechanical strength of the SRSP [40] (Fig. S1b).

Finally, the above components were thoroughly mixed and dispersed by wet chemical process for solvothermal treatment to form a homogeneous coating solution (Fig. 1a). The coating solution was subsequently cast onto pristine paper, and subjected to thermal curing, after which the surface changed from superhydrophilic to excellent superhydrophobic (Fig. 1b).

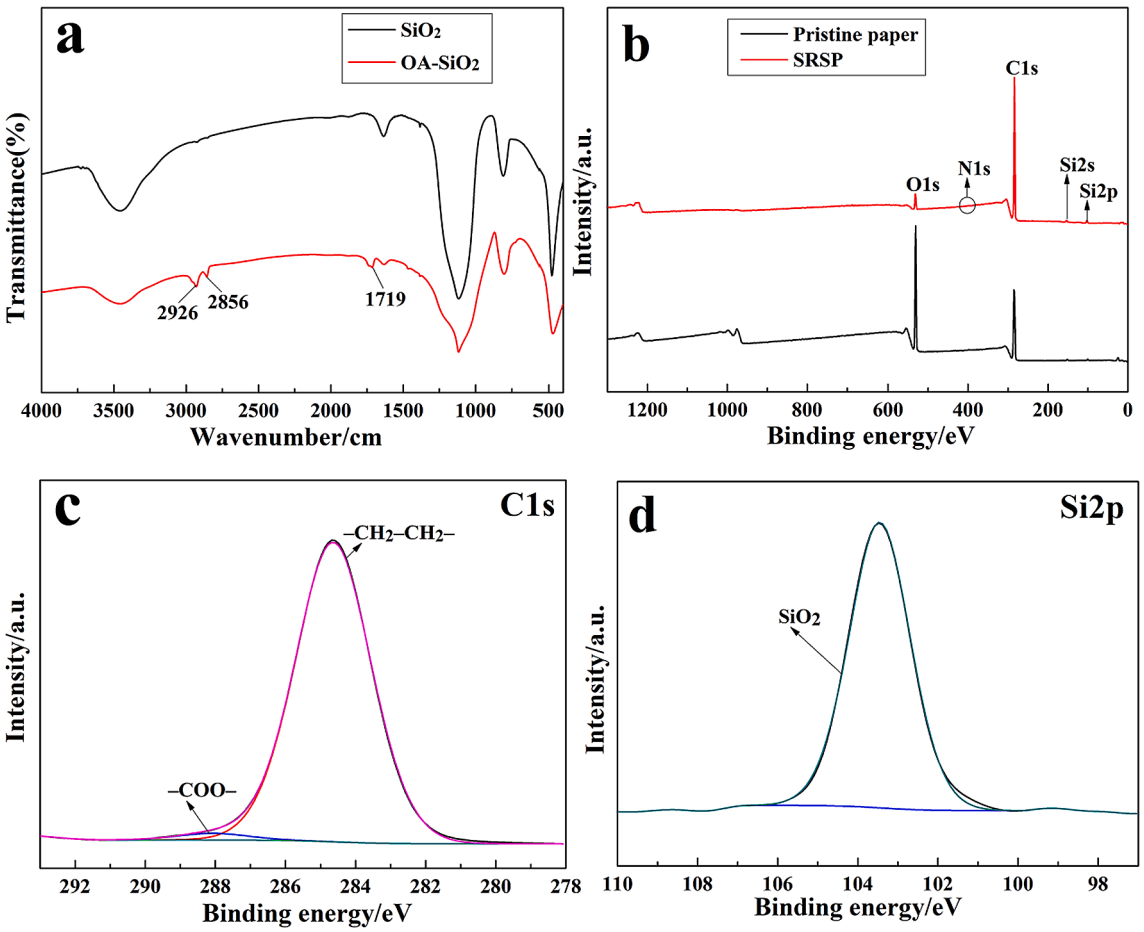


**Fig. 3. Characterization of surface composition.** (a) FTIR spectra of initial $SiO_2$ and OA-$SiO_2$ surfaces. (b) XPS survey spectra of pristine paper and SRSP. (c) C1s and (d) Si2p high-resolution XPS spectra on the SRSP surface.

Furthermore, the coating solution of SRSP is a composite coating composed of dispersed phase and continuous phase [38]. Polymers are widely used as continuous phases in such coatings, and, in our case, binder green mixed waxes were chosen as this phase. Dispersed phases are typically inorganic, such as $SiO_2$ or natural CNF. These high surface energy additives are commonly introduced as dispersed phases after alkylation treatment. In this study, we utilized green mixed wax as continuous phase to achieve higher bonding strength, which takes the advantages of multi-alkylated nanoparticles as well as green mixed waxes matrix as composite reinforcement system. As evident from Fig. 1c, the synergistic reinforcement of each component in our SRSP formula also imparts the strong interface binding force between coating molecules and the paper-based substrates, which provides an important guarantee for its durability.

### 3.2. *Surface morphology and chemical composition*

To understand the correlation between the surface morphology of samples and the corresponding wetting behavior, we performed SEM and AFM studies. The SEM image of the pristine paper composed of cellulose fibers displayed a microlevel rough surface and many fiber holes inside (Fig. 2a), facilitating the rapid spread of water droplets across the entire surface (Fig. 2b). In contrast, the surface of fiber in SRSP was covered with coating molecules, with significantly reduced surface pores. These coating molecules combined with inherent microlevel structures of the paper formed rough micro-/nanoscale hierarchical structures, which were irregularly and densely distributed on SRSP surface (Fig. 2c). Such a hierarchical topography composed of micro- and nanosized structures was mainly formed via the combination of hydrophobic nanoparticles, green binders and CNF, which provided the necessary structural basis for the superhydrophobic behavior of the SRSP surface. Unsurprisingly, it was observed that water droplets were not spread on the SRSP surface and remained a spherical shape with a CA of 156.8° (Fig. 2d). Furthermore, elemental mapping obtained using EDS confirmed that the SRSP surface was homogeneously covered with the nanocomposite (Fig. 2e), which suggested that the entire surface can be expected to show the same superhydrophobic behavior.

According to AFM images of SRSP surface, it was comprised predominantly of a rough hierarchical topography with surface roughness (Ra) values of 21.3 nm. Moreover, these surfaces displayed an uneven mountain-like structure, which quickly absorbed the air to form an air cushion, further confirming that the surface had a sufficiently rough structure, which highly resembled that of a lotus leaf surface and super-liquid-repellent properties (Fig. 2f).

To further investigate the liquid-repellency of the SRSP surface, the chemical composition was investigated using FTIR and XPS analysis. As exhibited in Fig. 3a, the absorption bands at 2926 and 2856 $cm^{-1}$ were attributed to the stretching vibration of C–H (–$CH_2$– and –$CH_3$) in the long alkyl chain of OA [41–43]. The other absorption bands at 1719 $cm^{-1}$ corresponded to the characteristic stretching vibration of C = O in carboxylic acid [41,43,44]. Thus, these results confirmed that the OA molecules were successfully grafted to $SiO_2$ nanoparticles through functional group reaction and electrostatic interactions.

In the wide survey XPS spectra, strong signals of C1s and O1s, and weak signals of Si2p, Si2s, and N1s were detected on SRSP surface. Fig. 3b compares the spectra of pristine paper and SRSP, where the atomic percentages of O and C atoms on SRSP surface decreased from 32.90% to 4.66%, and increased from 65.92% to 93.16%, respectively.

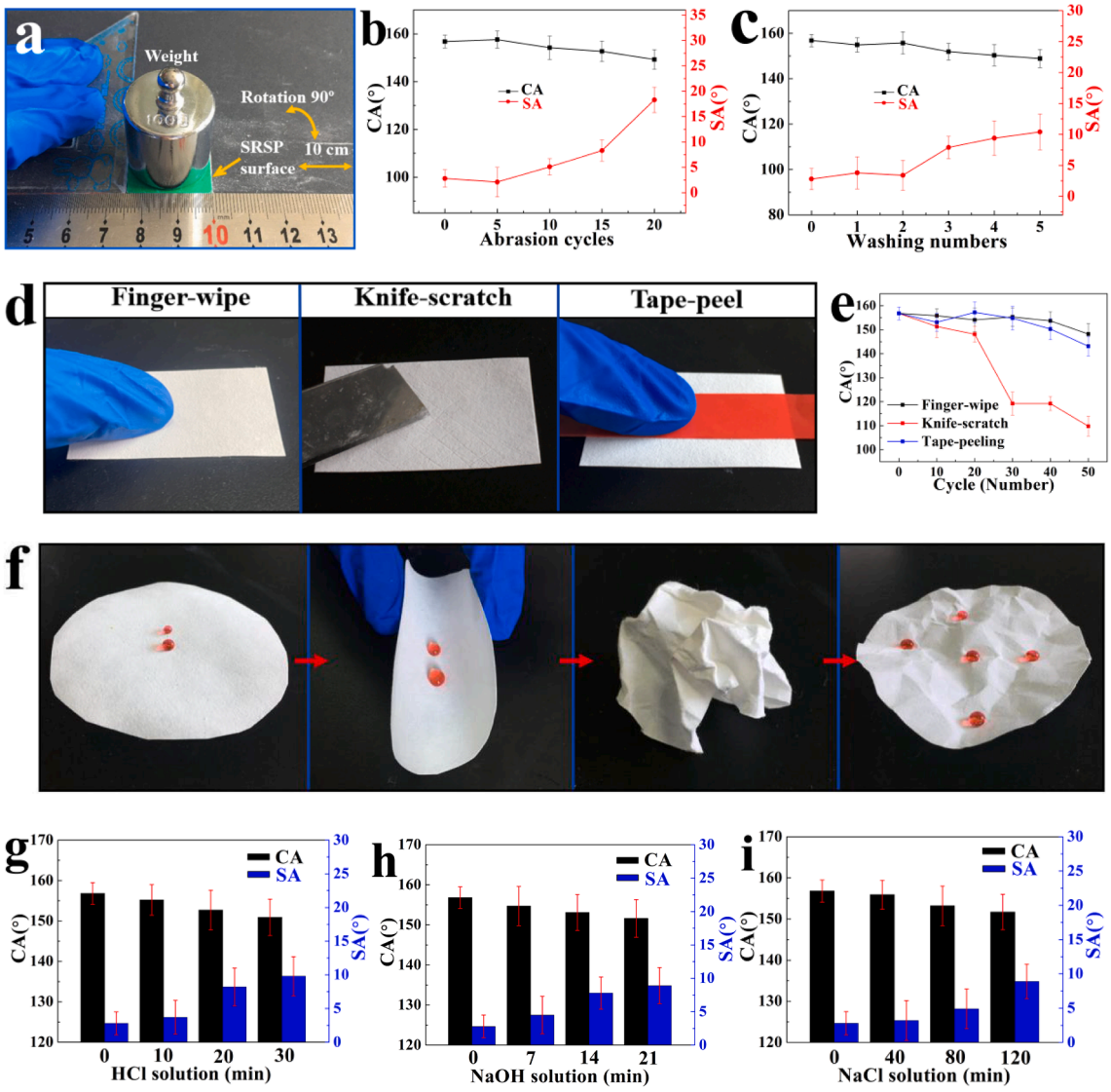


**Fig. 4. Mechanical robustness and chemical resistance of water-repellent SRSP surface.** (a) Schematic illustration of the abrasion test using sandpaper (one cycle). (b) CA and SA as a function of the mechanical abrasion cycle number for the SRSP surface. (c) CA and SA as a function of washing number for the SRSP surface. (d) Finger-wipe, knife-scratch, and tape-peeling tests to simulate practical handling conditions. (e) Durability test for the SRSP surface. (f) Bending and flexibility test of SRSP. (g-i) Change in CAs and SAs under different immersion time in HCl (0.05 M), NaOH (0.05 M), and NaCl (3.5 wt%) solutions, respectively.

That is, C1s/O1s intensity ratio increased significantly, indicating that the surface coating treatment resulted in increased C content on the surface of pristine paper, which was consistent with the chemical structure of OA and mixed waxes [37,45]. The high-resolution C1s peak of SRSP surface shown in Fig. 3c was deconvoluted into two photoelectron lines centered at approximately 284.6 eV and 288.3 eV and corresponded to $–CH_2–CH_2–$ and O–C = O, respectively [43,45,46]. Moreover, the Si2p peak located at 103.4 eV referred to $SiO_2$ (Fig. 3d) [45,47]. These results further demonstrated that OA and mixed waxes were successfully immobilized onto the surface of $SiO_2$, which together provided a low-surface-energy material basis for achieving superhydrophobicity of SRSP surface [34,37].

### 3.3. Mechanical and chemical durability

Durability is a key factor influencing the real-world applications of the superhydrophobic paper [4,48], and thus should be comprehensively taken into account. The results of different test types are presented in Fig. 4.

The sandpaper abrasion test is widely regarded as an effective route to evaluate the mechanical abrasion resistance of superhydrophobic surfaces [49]. Hence, we subjected the SRSP surface to an abrasive abrasion and measured in the presence of water CAs before and after exposure. As illustrated in Fig. 4a, the SRSP surface was placed downward on 800 mesh sandpaper in one direction under a load of 100 g (corresponding to a pressure of 1.6 kPa). It was moved 10 cm along the ruler back and forth, which was the equivalent of one abrasion cycle, guaranteeing that the surface was abraded longitudinally and transversely in each cycle. Fig. 4b shows the changes of CAs and SAs on the SRSP surfaces under different numbers of abrasion cycles. It was found that even after 17 abrasion cycles the water CAs consistently ranged between 156.8° and 150.7°, indicating that superhydrophobicity was retained. Notably, more abrasion cycles made it difficult for water to easily slip off the SRSP surface. According to visual observations, SA seemed more sensitive than the CA in measuring wettability of the sample after abrasion tests, increasing from 2.8° to 17.2°, which may be related to the breakage of some paper fibers. Further, the surface morphology after abrasion test was studied by SEM. After 5th and 15th abrasion cycle of SRSP surface, the hydrophobicity still exists although the micro/nano rough structure on the SRSP surface is partly damaged

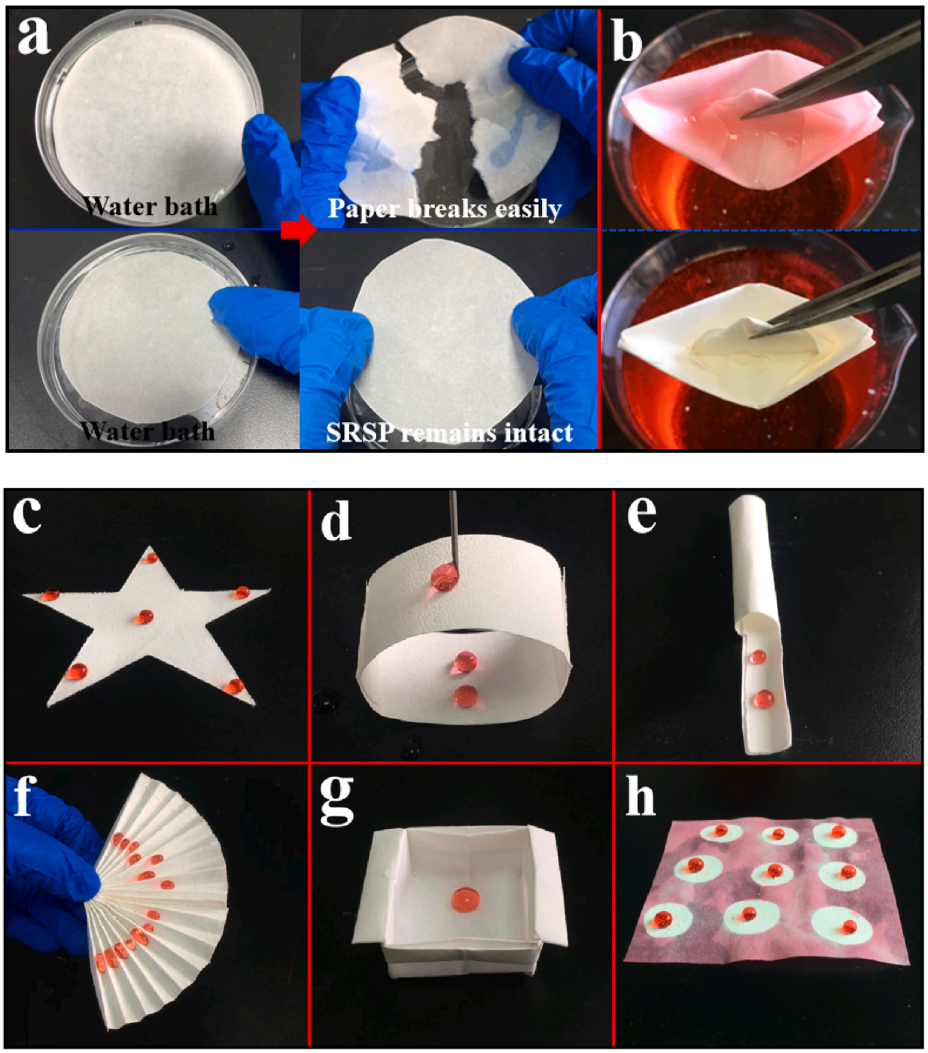


**Fig. 5. Integrity and flexibility of SRSP.** (a) Integrity of the fibers upon exposure to water for a longer time (the SRSP was compared with pristine paper). (b) Photos for the (top image) pristine paper and (bottom image) SRSP origami after being removed from red-colored water. (c) Water droplets deposited on star-shaped SRSP surface. (d-g) Optical images of water droplets on the various as prepared irregular shaped SRSP surfaces. (h) Optical images of water droplets on the pristine paper surface applied to a patterned surface with areas of different wettability on a single surface.

(Fig. S2a, b).

Additionally, when SRSP surface was exposed to a muddy water (soil-contaminated) mixture, and then washed continuously with a lab brush dipped in foul water four times, the surface maintained a water CA above 150° and SA below 10° (Fig. 4c). Furthermore, finger-wipe [38,50], the knife-scratch [7,38], tape-peeling [7,51], and sand/water impact [51,52] tests were also investigated on SRSP to simulate the various influences during practical application (Fig. 4d, Fig. S3a,b), and then plotted in Fig. 4e. To our delight, even after these harsh treatments, namely 45 times of wiping, 10 times of scratching, 40 cycles of peeling off, and sand/water impact from a height of 20 cm, SRSP surfaces still retained excellent superhydrophobicity with CAs of water exceeding 150°. In addition, as shown in Fig. 4f, SRSP was bent back and forth by hand and folded several times. It is worth noting that even when crumpled into a ball randomly and irregularly, no cracking, peeling or crumbling was observed on the surface, with droplets in the bent and wrinkled areas remaining as nearly perfect spheres. In particular, although there are clear scratches, the surface still has an visibly intact micro/nano rough structures after several times of bending and folding (Fig. S2c, d). The obtained results indicated that the prepared superhydrophobic coated paper was extremely resistant to damage caused by bending and wrinkling tests and had high mechanical flexibility and hydrophobic stability [9,53] .

In order to further study the durability of SRSP in more severe environments, CAs and SAs were observed after dipping them into HCl, NaOH, NaCl, and $H_2O$ solutions, and periodically removing the samples after rinsing with water and drying. Although such extremely harsh chemical corrosion is not very common in practice, it is a meaningful means to establish the SRSP chemical robustness [50,51]. The results are shown in Fig. 4g-i. SRSP maintained CA of above 150° after 30 min of acidic solution immersion (Fig. 4g), 21 min of alkaline solution immersion (Fig. 4h), 2 h of salt solution immersion (Fig. 4i), 120 h of water solution immersion (Fig. S3c), and even 240 h of UV light irradiation (Fig. S3d). At the same time, within experimental error, SA of ~ 10° or lower was maintained in all studied samples. These results confirmed that SRSP had good durability in chemical corrosion resistance.

Briefly, the above mentioned excellent durability was attributed to the multi-alkylation and the synergistic reinforcement strategy, which enabled SRSP surface to maintain its texture and hydrophobic components even while being degraded by external mechanical and chemical action. In terms of the material's perspective, the internal reason for reinforced damage resistance could stem from the selected green mixed waxes as adhesive molecules, so that while ensuring the superhydrophobicity of SRSP, it can not only enhance the inherent strength of the coating molecules, but also improve the adhesion with the paper substrate.

### 3.4. Key characteristic performance

Since pristine paper is a highly hydrophilic porous materials comprised of plant fiber as the main component, it is easily wetted by capillary action phenomenon, which has a huge effect on the strength

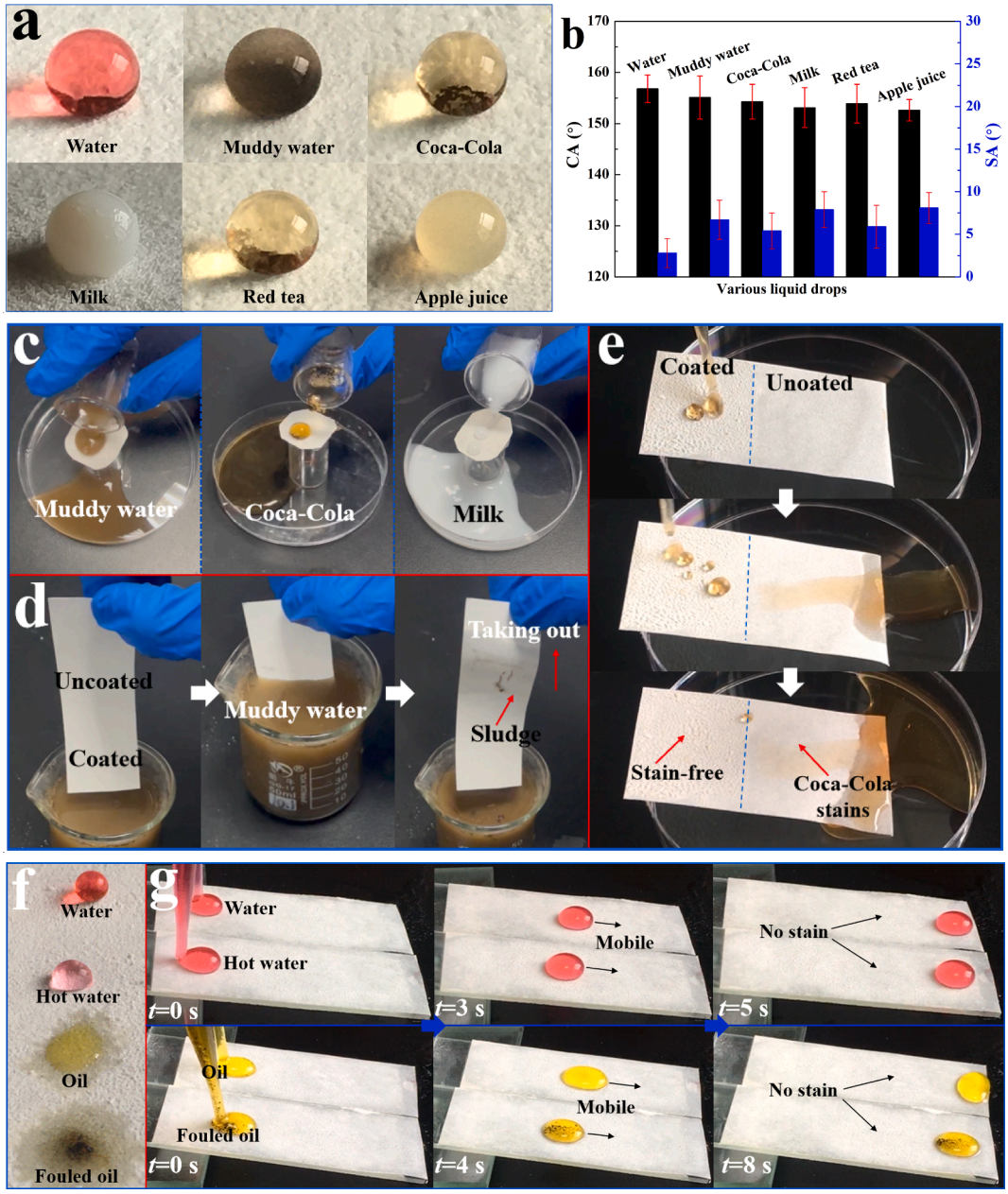


**Fig. 6. Direct antifouling ability of SRSP.** (a) Different types of liquid droplets with spherical shape on SRSP surface: red-colored water, muddy water, Coca-Cola, milk, red tea, and apple juice. (b) CAs and SAs of different liquids on the SRSP surface. (c) Three water-based liquids including muddy water, Coca-Cola, and milk were poured onto the SRSP surface. (d) Uncoated pristine paper surface (upper image) and SRSP surface (lower image) was dipped into muddy water and brought out. (e) Movement of Coca-Cola on the substrate composed of uncoated pristine paper surface (right) and SRSP surface (left). (f) Wetting behavior of water, hot-water (~100 °C), oil, and foul-oil droplets on SRSP surface. (g) Time-sequence images of the free mobility of water, hot-water, oil, and foul-oil droplets down along the tilted SLIPS-SRSP surfaces with a tile angle of ~ 10°.

and other integrity properties of paper, limiting its range of applications. In this case, in order to broaden the application scope to encompass currency notes, books, food packaging, thermal conductive pipe, paper-based electronic devices, microfluidic equipment, and medical diagnostic equipment, it is crucial that paper has exceptional water resistance [6,54,55].

Experiments illustrating this concept are demonstrated in Fig. 5, wherein the integrity of SRSP and the pristine paper were investigated by placing both in a water bath for the same period of time. After 20 min of water immersion, it was observed that the pristine paper was easily destroyed with the slightest touch. In contrast, the SRSP displayed excellent non-wetting behavior and remained intact envy after 5 days (Fig. 5a). In both cases, the force applied manually was similar (ignoring human error). In addition, when the blank filter paper was folded into the shape of a boat and completely soaked in dyed water, the boat was completely wetted and dyed red. On the other hand, the boat made of SRSP remained dry and showed no sign of the dye (Fig. 5b). The star-shaped pattern made of SRSP also retained the non-wetting state, as expected (Fig. 5c).

It is also worth noting that most superhydrophobic materials were constructed on the surface of flat substrates, and remains a major challenge to achieve superhydrophobicity on materials with irregular and special shapes [5,56]. In order to study the flexibility, SRSP was fabricated into different form factors such as 3D pipe, transfusion tube, 3D Chinese fan, and storage bag, respectively. Despite these irregular shapes being severely bent back and forth several times, contact angle

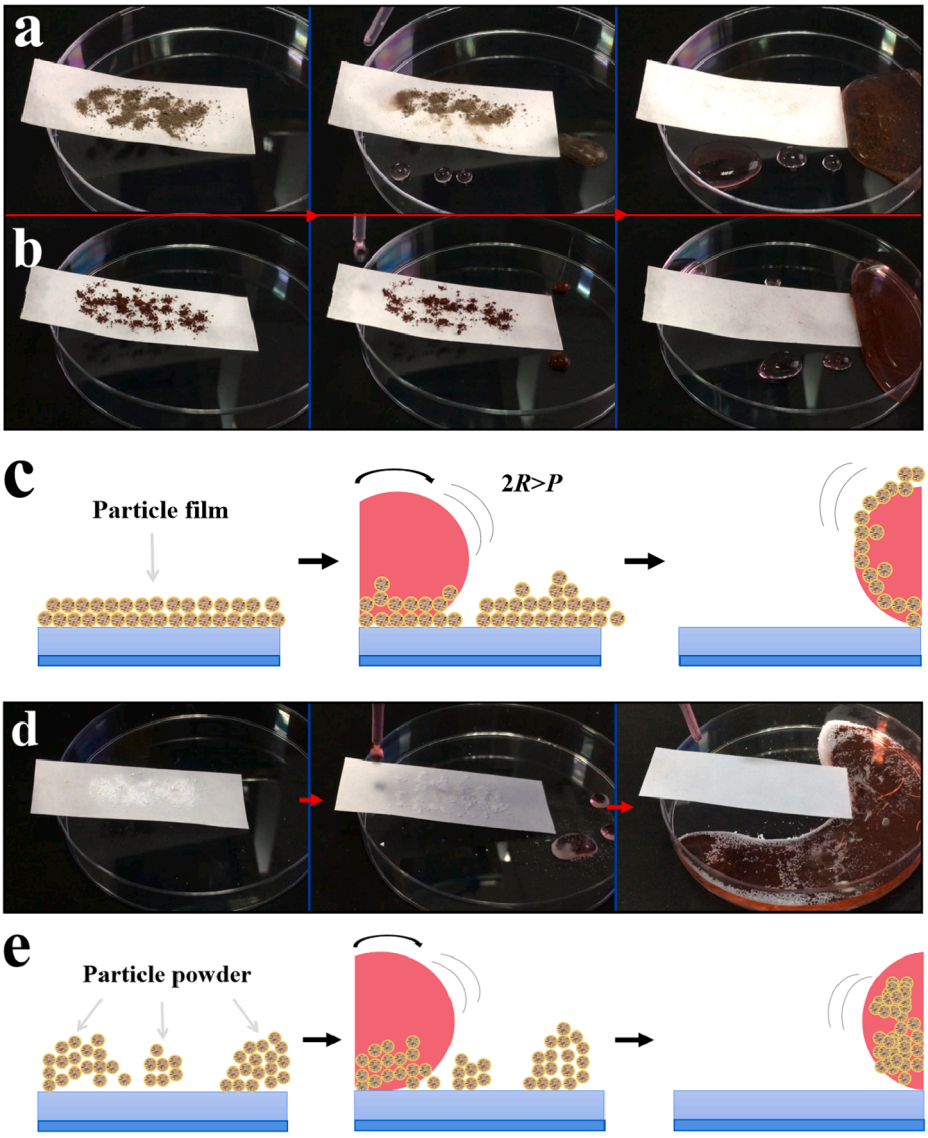


**Fig. 7. Indirect antifouling ability of SRSP.** (a, b) Hydrophilic particles (soil and $Fe_2O_3$ powder) were used as the model dirt/fouling agents. (c) Schematic illustration of the indirect antifouling process of hydrophilic particles (yellow; $2R > P$) by a water drop (red) on a SRSP surface (blue). (d) Hydrophobic $SiO_2$ particles were used as the model dirt/fouling agents. (e) Schematic illustration of the indirect antifouling process of hydrophobic particles (yellow) by a water drop (red).

measurements of these surfaces yielded near perfect spherical water drops with CA higher than 150° and no residue whatsoever was observed (Fig. 5d-g). Through a series of flexibility tests, it was further proved that SRSP had strong resistance to multiple bends. Furthermore, when pristine paper was prepared into patterned surface with different wettability values on a single paper substrate, no coating area showed superhydrophilicity, while the area coated with coating maintained the superhydrophobicity (Fig. 5h).

### 3.5. Antifouling functions

Antifouling ability is a critical index for superhydrophobic paper when considering practical applications [9,57]. Based on the different modes of surface decontamination, we divided antifouling ability into direct and indirect antifouling ability. As displayed in Fig. 6a, SRSP surface was not contaminated by water-based liquids in life regardless of the color, viscosity and composition, such as clear water, muddy water, Coca-Cola, milk, red tea, and apple juice. It was found that these droplets easily rolled off SRSP surface without leaving a trace due to low SA < 5° and high CA > 150° (Fig. 6b). Thus, it was clear that the superhydrophobic capacity endowed SRSP with excellent repellency towards a variety of liquids.

To evaluate direct antifouling ability, we poured three water-based liquids onto the SRSP surface. In all the experiments, the liquids easily rolled off the horizontal SRSP surface without any trace, not only transparent liquids (Coca-Cola) but also suspensions and emulsions (muddy water, and milk) (Fig. 6c and video S1). In addition, the sample was immersed in sewage consisting of soil and sand for several seconds. Upon removal from the test liquids, the surface of SRSP part remained as clean as before even after repeated immersion in muddy water, while the surface of uncoated paper part as the control was wetted or smudged (Fig. 6d and video S1). Furthermore, the liquids flowed down and removed solid contaminants from SRSP surface. Similarly, it was also clearly observed that Coca-Cola tended to easily slide down from SRSP surface without any liquid residue, but rapidly wetted and stained the uncoated paper surface (Fig. 6e). These phenomena were attributed to the existence of abundant micro-/nanopores on SRSP surface (Fig. 2c), which facilitated trapping air, and promoted excellent direct antifouling behavior against water-based liquids.

Furthermore, slippery liquid (silicone oil) was infused into the

porous structure of SRSP to obtain the SLIPS-SRSP [38,58]. As observed with camera imaging, the SRSP surface retained its super-repellency for water droplets and pinning for low-surface-energy droplets (hot-water, oil, and fouled oil) (Fig. 6f). Interestingly, these low-surface-energy droplets contacted SLIPS-SRSP surface without leaving any traces, and easily slid down its surface, confirming its excellent anti-adhesion performance (Fig. 6g).

In order to further demonstrate the indirect antifouling ability (that is, self-cleaning ability), we used soil/iron oxide ($Fe_2O_3$) powder with the particle diameter ($2R$) larger than SRSP pore diameter ($P$) as a model foulant of hydrophilic particles in the field of environmental engineering [59]. As expected, the water droplets that rolled off removed contaminants, leaving behind a clean track suggesting weak interaction between the liquid droplets and coating (Fig. 7a-c and video S2). Then, to mimic common hydrophobic contamination sources, such as dust or soot, we applied hydrophobic $SiO_2$ particle powders to SRSP surface. After contaminating the surface with the particle powders, the adsorbed $SiO_2$ particles were almost eliminated through the contact of water droplets with the surface, indicating that even nanoscopic hydrophobic particle powders did not hamper the superhydrophobicity of SRSP surface (Fig. 7d,e and video S2).

These phenomena were consistent with the "lotus effect" and could be attributed to the surface coating with well-designed nano- or micrometer-sized protrusions possessing an entrapped layer of air around them to form a so-called Cassie state [60], thereby protecting the surface from contamination [61–63]. These outstanding indirect antifouling properties of SRSP showed great promise for long-term industrial applications in harsh environments.

## 4. Conclusions

In summary, we presented a simple strategy to develop durable SRSP using fluorine-free raw materials. The synergistic effect between the green-based adhesives and hydrophobic $SiO_2$ nanoparticles was responsible for the enhanced durability of SRSP that demonstrated liquid repellency even after subjection to a variety of testing conditions (sandpaper abrasion, finger-wipe, knife-scratch, tape-peel, and bending) and chemical damage (strong acid/base attack). Notably, SRSP showed superior direct/indirect antifouling ability towards various foulants, including muddy water, Coca-Cola, milk, red tea, apple juice, and hydrophilic/hydrophobic particles. In particular, silicone oil was infused into the micro/nanoscale structured SRSP to obtain the SLIPS-SRSP surface, which exhibited remarkable non-fouling activity against hot water, oil, and fouled oil, thereby enhancing the functional performance of the surface. Besides, through a series of flexibility tests, it was further confirmed that SRSP has strong resistance to multiple bends. Finally, we envision that such superhydrophobic paper, which is harmless to the environment and human benign, can potentially be used for industrial and medical fields, and provide a basis for its applications in different paper-based technologies.

### *CRediT authorship contribution statement*

**Cai Long:** Data curation, Formal analysis, Writing – original draft. **Yongquan Qing:** Conceptualization, Methodology, Supervision, Funding acquisition. **Xiao Long:** Data curation, Investigation. **Niu Liu:** Visualization, Investigation. **Xinyu Xu:** Validation, Investigation. **Kai An:** Investigation. **Mengxue Han:** Validation. **Songhe Li:** Project administration. **Changsheng Liu:** Writing – review & editing.

### Declaration of Competing Interest

The authors declare that they have no known competing financial interests or personal relationships that could have appeared to influence the work reported in this paper.

### Acknowledgements

This work was supported by the Fundamental Research Funds for the Central Universities (2020GFYD006), National Natural Science - Foundation of China (52001062), and Opening Project of State Key Laboratory of Light Alloy Casting Technology for High-end Equipment and Natural Science Foundation of Liaoning Province (2020-KF-14-02).

### Appendix A. Supplementary material

Supplementary data to this article can be found online at https://doi.org/10.1016/j.apsusc.2021.152144.

### References

[1] L. Peng, Y. Meng, H. Li, Facile fabrication of superhydrophobic paper with improved physical strength by a novel layer-by-layer assembly of polyelectrolytes and lignosulfonates-amine, Cellulose 23 (3) (2016) 2073–2085.
[2] G. Wen, X. Gao, P. Tian, L. Zhong, Z. Wang, Z. Guo, Modifier-free fabrication of durable and multifunctional superhydrophobic paper with thermostability and anti-microbial property, Chem. Eng. J. 346 (2018) 94–103.
[3] T. Arbatan, L. Zhang, X.-Y. Fang, W. Shen, Cellulose nanofibers as binder for fabrication of superhydrophobic paper, Chem. Eng. J. 210 (2012) 74–79.
[4] Q. Wang, D. Xie, J. Chen, G. Liu, M. Yu, Facile fabrication of superhydrophobic and photoluminescent TEMPO-oxidized cellulose-based paper for anticounterfeiting application, ACS Sustain. Chem. Eng. J. 8 (35) (2020) 13176–13184.
[5] J. Li, J. Tian, Y. Gao, R. Qin, H. Pi, M. Li, P. Yang, All-natural superhydrophobic coating for packaging and blood-repelling materials, Chem. Eng. J. 410 (2021), 128347.
[6] A. Baidya, M.A. Ganayee, S. Jakka Ravindran, K.C. Tam, S.K. Das, R.H.A. Ras, T. Pradeep, Organic solvent-free fabrication of durable and multifunctional superhydrophobic paper from waterborne fluorinated cellulose nanofiber building blocks, ACS Nano 11 (11) (2017) 11091–11099.
[7] F.-F. Chen, Z.-H. Dai, Y.-N. Feng, Z.-C. Xiong, Y.-J. Zhu, Y. Yu, Customized cellulose fiber paper enabled by an in situ growth of ultralong hydroxyapatite nanowires, ACS Nano 15 (3) (2021) 5355–5365.
[8] M. Wang, Z. Zhang, Y. Wang, X. Zhao, M. Yang, X. Men, Q. Xue, Colorful superhydrophobic pigments with superior anti-fouling performance and environmental durability, Chem. Eng. J. 384 (2020), 123292.
[9] Y. Teng, Y. Wang, B. Shi, X. Li, Y. Chen, Robust superhydrophobic surface fabrication by fluorine-free method on filter paper for oil/water separation, Polym. Test. 91 (2020), 106810.
[10] G. Chitnis, Z. Ding, C.L. Chang, C.A. Savran, B. Ziaie, Laser-treated hydrophobic paper: an inexpensive microfluidic platform, Lab chip 11 (6) (2011) 1161–1165.
[11] Z.Y. Yang, H.M. Liu, Y. Tian, Y. Chen, Z. Niu, C. Zhou, C.L. Zhou, F.Y. Wang, C. J. Gu, S.W. Tang, T. Jiang, J. Zhou, Synergistic effect of a "stellate" mesoporous $SiO_2$@ Au nanoprobe and coffee-ring-free hydrophilic–hydrophobic substrate assembly in an ultrasensitive SERS-based immunoassay for a tumor marker, J. Mater. Chem. C 8 (6) (2020) 2142–2154.
[12] X. Tian, T. Verho, R.H.A. Ras, Moving Superhydrophobic Surfaces Toward Real-World Applications, Science 352 (6282) (2016) 142–143.
[13] H. Zhou, Y. Zhao, H. Wang, T. Lin, Recent Development in Durable Super-Liquid-Repellent Fabrics, Adv. Mater. Interfaces 3 (2016) 1600402.
[14] B. Zhang, W. Xu, Q. Zhu, Y. Sun, Y. Li, Mechanically robust superhydrophobic porous anodized AA5083 for marine corrosion protection, Corros. Sci. 158 (2019), 108083.
[15] S. Jiang, S. Zhou, B. Du, R. Luo, Preparation of superhydrophobic paper with double-size silica particles modified by amino and epoxy groups, AIP Adv. 11 (2021), 025127.
[16] E. Ahn, T. Kim, Y. Jeon, B.S. Kim, A4 paper chemistry: synthesis of a versatile and chemically modifiable cellulose membrane, ACS Nano 14 (2020) 6173–6180.
[17] G. Chen, P. Zhu, Y. Kuang, Y.u. Liu, D. Lin, C. Peng, Z. Wen, Z. Fang, Durable superhydrophobic paper enabled by surface sizing of starch-based composite films, Appl. Surf. Sci. 409 (2017) 45–51.
[18] A. Geissler, F. Loyal, M. Biesalski, K. Zhang, Thermo-responsive superhydrophobic paper using nanostructured cellulose stearoyl ester, Cellulose 21 (1) (2014) 357–366.
[19] P. Mohammadi, G. Beaune, B.T. Stokke, J.V. Timonen, M.B. Linder, Self-coacervation of a silk-like protein and its use as an adhesive for cellulosic materials, ACS Macro Lett. 7 (2018) 1120–1125.
[20] W. Zhang, P. Lu, L. Qian, H. Xiao, Fabrication of superhydrophobic paper surface via wax mixture coating, Chem. Eng. J. 250 (2014) 431–436.
[21] P. Khanjani, A.W.T. King, G.J. Partl, L.-S. Johansson, M.A. Kostiainen, R.H.A. Ras, Superhydrophobic paper from nanostructured fluorinated cellulose esters, ACS Appl. Mater. Interfaces 10 (13) (2018) 11280–11288.
[22] Z. Li, Y. Xing, J. Dai, Superhydrophobic surfaces prepared from water glass and non-fluorinated alkylsilane on cotton substrates, Appl. Surf. Sci. 254 (7) (2008) 2131–2135.

[23] C. Cao, M. Ge, J. Huang, S. Li, S. Deng, S. Zhang, Y. Lai, Robust flfluorine-free superhydrophobic PDMS–ormosil@fabrics for highly effffective self-cleaning and effiffifficient oil–water separation, J. Mater. Chem. A 4 (2016) 12179–12187.

[24] T.M. Schutzius, I.S. Bayer, J. Qin, D. Waldroup, C.M. Megaridis, Water-based, nonflfluorinated dispersions for environmentally benign, large-area, superhydrophobic coatings, ACS Appl. Mater. Interfaces 5 (2013) 13419–13425.

[25] H. Ogihara, J. Xie, J. Okagaki, T. Saji, Simple method for preparing superhydrophobic paper: spray-deposited hydrophobic silica nanoparticle coatings exhibit high water-repellency and transparency, Langmuir 28 (2012) 4605–4608.

[26] B. Zhang, Q. Zhu, Y. Li, B. Hou, Facile fluorine-free one step fabrication of superhydrophobic aluminum surface towards self-cleaning and marine anticorrosion, Chem. Eng. J. 352 (2018) 625–633.

[27] T. Darmanin, F. Guittard, Superoleophobic surfaces with short fluorinated chains, Soft Matter 9 (25) (2013) 5982, https://doi.org/10.1039/c3sm50643f.

[28] Y. Si, Z. Guo, Eco-friendly functionalized superhydrophobic recycled paper with enhanced flame-retardancy, J. Colloid Interface Sci. 477 (2016) 74–82.

[29] X. Liu, X. Zhang, Q. Chen, Y. Pan, C. Liu, C. Shen, A simple superhydrophobic/superhydrophilic Janus-paper with enhanced biocompatibility by PDMS and candle soot coating for actuator, Chem. Eng. J. 406 (2021), 126532.

[30] X. Zhong, J. Sheng, H. Fu, A novel UV/sunlight-curable anti-smudge coating system for various substrates, Chem. Eng. J. 345 (2018) 659–668.

[31] Z. Li, M. Rabnawaz, Fabrication of food-safe water-resistant paper coatings using a melamine primer and polysiloxane outer layer, ACS Omega 3 (9) (2018) 11909–11916.

[32] C. Spathi, N. Young, J.Y.Y. Heng, L.J.M. Vandeperre, C.R. Cheeseman, A simple method for preparing super-hydrophobic powder from paper sludge ash, Mater. Lett. 142 (2015) 80–83.

[33] Z. Hu, X. Zen, J. Gong, Y. Deng, Water resistance improvement of paper by superhydrophobic modification with microsized $CaCO_3$ and fatty acid coating, Colloid. Surface. A 351 (1-3) (2009) 65–70.

[34] W. Wang, K. Lockwood, L.M. Boyd, M.D. Davidson, S. Movafaghi, H. Vahabi, S. R. Khetani, A.K. Kota, Superhydrophobic coatings with edible materials, ACS Appl. Mater. Interfaces 8 (29) (2016) 18664–18668.

[35] Ç. Koşak Söz, S. Trosien, M. Biesalski, Superhydrophobic hybrid paper sheets with Janus-type wettability, ACS Appl, Mater. Interfaces 10 (43) (2018) 37478–37488.

[36] I.S. Bayer, Superhydrophobic coatings from ecofriendly materials and processes: a review, Adv. Mater. Interfaces 7 (13) (2020) 2000095, https://doi.org/10.1002/admi.v7.1310.1002/admi.202000095.

[37] B.-Y. Liu, C.-H. Xue, Q.-F. An, S.-T. Jia, M.-M. Xu, Fabrication of superhydrophobic coatings with edible materials for super-repelling non-Newtonian liquid foods, Chem. Eng. J. 371 (2019) 833–841.

[38] C. Long, Y.Q. Qing, K. An, X. Long, C. Liu, S. Shang, C.S. Liu, Functional fluorination agents for opposite extreme wettability coatings with robustness, water splash inhibition, and controllable oil transport, Chem. Eng. J. 415 (2021), 128895.

[39] M. Rabnawaz, G. Liu, H. Hu, Fluorine-free anti-smudge polyurethane coatings, Angew. Chem. Int. Ed. 127 (43) (2015) 12913–12918.

[40] L. Lai, J. Li, P. Liu, L. Wu, S.J. Severtson, W.J. Wang, Mechanically reinforced biodegradable Poly(butylene adipate-co-terephthalate) with interactive nanoinclusions, Polymer 197 (2020), 122518.

[41] N. Rakhshan, M. Pakizeh, Removal of triazines from water using a novel OA modified $SiO_2$/PA/PSf nanocomposite membrane, Sep. Purif. Technol. 147 (2015) 245–256.

[42] J. Liu, X. Li, W. Jia, Z. Li, Y. Zhao, S. Ren, Demulsification of crude oil-in-water emulsions driven by graphene oxide nanosheets, Energ, Fuel. 29 (7) (2015) 4644–4653.

[43] S. Javadian, Magnetic superhydrophobic polyurethane sponge loaded with $Fe_3O_4$@oleic acid@graphene oxide as high performance adsorbent oil from water, Chem. Eng. J. 408 (2021), 127369.

[44] M.Z. Kassaee, E. Motamedi, M. Majdi, Magnetic $Fe_3O_4$-graphene oxide/polystyrene: fabrication and characterization of a promising nanocomposite, Chem. Eng. J. 172 (2011) 540–549.

[45] L. Wang, K.G. Neoh, E.-T. Kang, B. Shuter, Multifunctional polyglycerol-grafted $Fe_3O_4$@ $SiO_2$ nanoparticles for targeting ovarian cancer cells, Biomaterials 32 (8) (2011) 2166–2173.

[46] G. Xie, P. Xi, H. Liu, F. Chen, L. Huang, Y. Shi, F. Hou, Z. Zeng, C. Shao, J. Wang, A facile chemical method to produce superparamagnetic graphene oxide–$Fe_3O_4$ hybrid composite and its application in the removal of dyes from aqueous solution, J. Mater. Chem. 22 (3) (2012) 1033–1039.

[47] Z. Cheng, H. Lai, Y. Du, K. Fu, R. Hou, N. Zhang, K. Sun, Underwater superoleophilic to superoleophobic wetting control on the nanostructured copper substrates, ACS Appl. Mater. Interfaces 5 (21) (2013) 11363–11370.

[48] H. Li, X. Wang, Y. He, L. Peng, Facile preparation of fluorine-free superhydrophobic/superoleophilic paper via layer-by-layer deposition for self-cleaning and oil/water separation, Cellulose 26 (3) (2019) 2055–2074.

[49] Y. Lu, S. Sathasivam, J. Song, C.R. Crick, C.J. Carmalt, I.P. Parkin, Robust self-cleaning surfaces that function when exposed to either air or oil, Science 347 (6226) (2015) 1132–1135.

[50] Y. Qing, C. Yang, N. Yu, Y. Shang, Y. Sun, L. Wang, C. Liu, Superhydrophobic $TiO_2$/polyvinylidene fluoride composite surface with reversible wettability switching and corrosion resistance, Chem. Eng. J. 290 (2016) 37–44.

[51] C. Peng, Z. Chen, M.K. Tiwari, All-organic superhydrophobic coatings with mechanochemical robustness and liquid impalement resistance, Nat. Mater. 17 (4) (2018) 355–360.

[52] X. Deng, L. Mammen, H.J. Butt, D. Vollmer, Candle soot as a template for a transparent robust superamphiphobic coating, Science 335 (2012) 67–70.

[53] X. Zhang, Z. Liu, Y. Li, C. Wang, Y. Zhu, H. Wang, J. Wang, Robust superhydrophobic epoxy composite coating prepared by dual interfacial enhancement, Chem. Eng. J. 371 (2019) 276–285.

[54] A.S. Anjum, K.C. Sun, M. Ali, R. Riaz, S.H. Jeong, Fabrication of coral-reef structured nano silica for self-cleaning and super-hydrophobic textile applications, Chem. Eng. J. 401 (2020), 125859.

[55] X. Hou, Y.S. Zhang, G. Trujillo-de Santiago, M.M. Alvarez, J. Ribas, S.J. Jonas, A. Khademhosseini, Interplay between materials and microfluidics, Nat. Rev. Mater. 2 (2017) 1–15.

[56] S.S. Latthe, R.S. Sutar, A.K. Bhosale, S. Nagappan, C. Ha, K.K. Sadasivuni, S. Liu, R. Xing, Recent developments in air-trapped superhydrophobic and liquid-infused slippery surfaces for anti-icing application, Prog. Org. Coat. 137 (2019) 105373–105381.

[57] Q.i. Li, Z. Guo, A highly fluorinated $SiO_2$ particle assembled, durable superhydrophobic and superoleophobic coating for both hard and soft materials, Nanoscale 11 (39) (2019) 18338–18346.

[58] T.-S. Wong, S.H. Kang, S.K.Y. Tang, E.J. Smythe, B.D. Hatton, A. Grinthal, J. Aizenberg, Bioinspired self-repairing slippery surfaces with pressure-stable omniphobicity, Nature 477 (7365) (2011) 443–447.

[59] F. Geyer, M. D'Acunzi, A. Sharifi-Aghili, A. Saal, N. Gao, A. Kaltbeitzel, T.-F. Sloot, R. Berger, H.-J. Butt, D. Vollmer, When and how self-cleaning of superhydrophobic surfaces works, Sci. Adv. 6 (3) (2020), https://doi.org/10.1126/sciadv.aaw9727.

[60] A.B.D. Cassie, S. Baxter, Wettability of porous surfaces, Trans. Faraday Soc. 40 (1944) 546–551.

[61] X. Ou, J. Cai, J. Tian, B. Luo, M. Liu, Superamphiphobic surfaces with self-cleaning and antifouling properties by functionalized chitin nanocrystals, ACS Sustain. Chem. Eng. 8 (17) (2020) 6690–6699.

[62] S.L. Zheng, D.A. Bellido-Aguilar, X.H. Wu, X.J. Zhan, Y.J. Huang, X.T. Zeng, Q. C. Zhang, Z. Chen, Durable waterborne hydrophobic bio-epoxy coating with improved anti-icing and self-cleaning performance, ACS Sustain. Chem. Eng. J. 7 (2019) 641–649.

[63] L. Chen, Z. Guo, W. Liu, Biomimetic multi-functional superamphiphobic FOTS-$TiO_2$ particles beyond lotus leaf, ACS Appl. Mater. Interfaces 8 (2016) 27188–27198.